

# STATUS AND CHALLENGES AT TRIUMF ISAC FACILITY\*

Z. Yao<sup>†</sup>, Z. Ang, T. Au, K. Fong, X. Fu, J.J. Keir, P. Kolb, D. Lang, R.E. Laxdal, R. Leewe, Y. Ma, B. Matheson, R.S. Sekhon, B.S. Waraich, Q. Zheng, V. Zvyagintsev, TRIUMF, Vancouver, Canada

## Abstract

The ISAC facility uses the ISOL technique to produce radioactive ions for experiments. The post-accelerator consists of a room temperature linac (ISAC-I) and a superconducting linac (ISAC-II). After more than two decades of beam delivery in ISAC, the RF systems have met various challenges regarding increased operation requirements, system stability issues and performance improvements. This paper discusses the detailed challenges in recent years in both ISAC-I and ISAC-II. The upgrade plan or mitigation solution to address each challenge is reported respectively. A hint of the long-term vision at ISAC is also briefly described at the end of the paper.

## INTRODUCTION

The Isotope Separator and ACcelerator (ISAC) at TRIUMF (see Fig. 1) uses the Isotope Separation On-Line (ISOL) technique to produce rare-isotope beams (RIB) for studies in astrophysics, nuclear structure and reactions, electroweak interactions and material science [1]. RIB production consists of a 500 MeV cyclotron producing a proton driver beam of up to 100  $\mu$ A onto one of two thick production targets, an on-line ion source and a mass-separator. The radioactive ions are accelerated in a chain of linear accelerators (linac) consisting of a room temperature RFQ and DTL to an energy of 1.5 MeV/u and a superconducting linac that adds a further 40 MV to the beam for nuclear physics investigations near the Coulomb barrier.

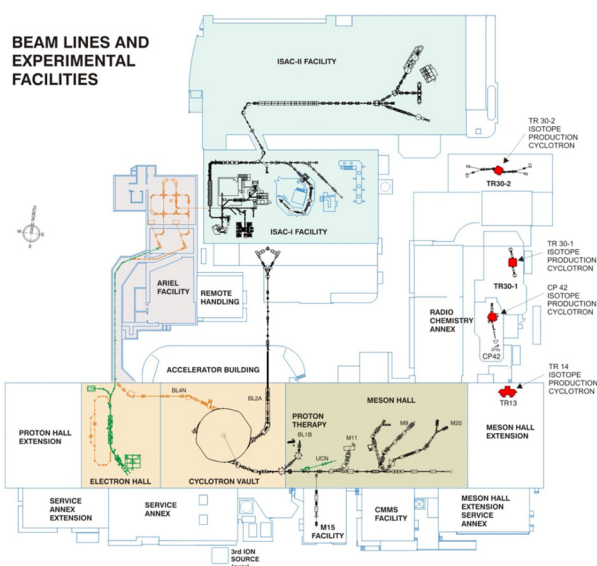


Figure 1: TRIUMF accelerator complex.

\*TRIUMF receives funding via a contribution through the National Research Council Canada

<sup>†</sup>zyyao@triumf.ca

The ARIEL project [1] is a new RIB production facility at TRIUMF under construction. An additional 100  $\mu$ A proton beam will be extracted from the main cyclotron and delivered to the 50 kW proton target of ARIEL. A new 1.3 GHz electron linac (e-Linac) will provide a 30 MeV electron beam with the average beam power up to 100 kW to the other electron converter target in the same target hall. The two ARIEL targets will add two RIBs and triple the RIB availability by delivering three simultaneous beams to ISAC. The e-Linac recently achieved 10 kW average beam power to a high power beam dump at the beam energy of 30 MeV during beam commissioning.

## ISAC-I CHALLENGES

ISAC-I is the room temperature linac for RIB acceleration. It consists of 18 continuous-wave (CW) RF systems, with operating frequency ranges from 5.89 MHz to 106.08 MHz and RF power specified up to 90 kW. The first accelerator in ISAC-I is a 35.36 MHz split-ring, four-vane Radio Frequency Quadrupole (RFQ), designed without a gentle buncher or buncher section. The RFQ focusses and accelerates RIB from 2.04 keV/u ( $\beta = 0.0021$ ) to 153 keV/u with a mass-to-charge ratio of  $A/q \leq 30$  [2]. A post-stripper, 106.08 MHz variable energy drift tube linac (DTL) accelerates ions of  $3 \leq A/q \leq 6$  to a final energy from 0.15 MeV/u to 1.53 MeV/u. The DTL structure has been configured as a separated function DTL [3]. Five independently phased IH tanks operating at  $\phi_s = 0^\circ$  provide the main acceleration. Longitudinal focussing is provided by independently phased, triple gap, split-ring resonator structures positioned before the second, third and fourth IH tanks. Quadrupole triplets placed after each IH tank maintain transverse focussing. The ISAC-I linac has been accelerating RIBs and stable beams for experiments since 2000.

## RF Amplifier

The demand of the accelerated RIBs at ISAC has been growing over the years. Manual re-phasing by operators is required to accommodate daily changes in energy and isotope species. Beam tuning is accomplished by turning off all RF systems and then setting up the amplitude and the phase of each RF system in the sequence from the upstream to the downstream. To minimize the re-phasing time, RF systems are required to ramp up from the 'OFF' state to the high-power state and to stabilize in the operating regime in a short time.

The tube amplifiers intrinsically require time for warmup and stabilization as the tube and RF circuits are heated by RF power. ISAC-I tube amplifiers have been in operation for over 20 years. The aged matching circuit in the tetrode tube amplifiers extends the warmup process, which challenges the beam delivery requirements. Blowing warm air was applied to pre-warm the matching circuit

as a temporary mitigation solution. The aged tube amplifiers have also been prone to the overheating issue of the tube sockets. It causes system trips and RF downtime. In addition, obsolete tubes being used in ISAC-I enhances the challenge of system maintenance.

Solid-state amplifier (SS Amp) technology has been fast developed in the past decade. The capital costs of SS Amps for ISAC-I system are now comparable to tube amplifiers. There are several advantages: 1) Considering the long lifetime of SS Amps, the long-term maintenance cost is less, 2) SS Amps have better phase stability in the warmup or the normal operating regime can accommodate fast beam setup, 3) the high gain of SS Amps eliminates the required driver in the tube amplifier, 4) the matching issue between the driver and the final stage is removed, 5) SS Amp is integrated with modules, which is easier for the troubleshooting, and 6) the replacement requires less RF circuit knowledge for maintenance on the personnel training aspect.

As a long-term project TRIUMF has planned to replace all the tube amplifiers in ISAC-I by SS Amps. The 106 MHz 4.8 kW SS Amp was installed and commissioned for the bunch rotator in 2022 winter shutdown. The next replacement will be DTL tank4. The 106 MHz 25 kW SS Amp is in production and is to be installed in 2023. Other systems will be upgraded gradually in the future, while the DTL tanks have the highest priority.

### *Low-Level RF (LLRF)*

The beam delivery over a broad range of A/q requires RF systems to operate in a large dynamic range of RF power. In the high A/q regime, the high-power RF is challenging as discussed above. As a contrast, in the extreme low power regime, resonators could see multipacting (MP) barriers and show instability in the operation. In addition, the hybrid LLRF system designed in the 1990s brings more challenges to the low power regime operation. LLRF is optimized for the full power operation. The hybrid system has a non-linear response out of the dynamic range. The saturation regime in the higher end is not reached during operation. But the lower non-linear regime makes the scaling of RF setpoints inaccurate. There are offsets in the hybrid boards, which allow a non-zero output for a zero setting. And the various offsets between systems makes the beam tuning more complicated in the low power regime and requires more effort from the operator.

To address the issue of the hybrid LLRF and provide identical control for RF systems, an FPGA based fully digital LLRF has been developed with high-speed ADC and DAC [4] for the ISAC-I LLRF upgrade project. The first digital LLRF, based on the VXI mainframe, was designed for the ARIEL pre-buncher powered by a sawtooth waveform which is the combination of the three harmonics of 11.79 MHz. The system was also employed in the ISAC pre-buncher and ISAC booster in 2019. The remaining systems in ISAC-I will be upgraded to the digital LLRF by 2023. The manufacture of the control boards has been completed. The new systems will be assembled and tested soon. The new LLRF provides an on-board communication

interface with the control computer, to avoid the increasing maintenance cost of the VXI mainframe due to the obsolete key components. The new LLRF system will be integrated in a NIM crate, which is a long-lasting technology.

### *Phase Stability*

Beam delivery experts have observed DTL beam transmission changes between day and night. The transmission drift typically requires a few degrees of adjustment of the synchronizing phase to restore transmission. The phase drifts were measured systematically on the reference signal. The problematic location was determined to be between the control consoles of the RFQ and DTL. The five DTL tanks are controlled by two RF control stations. Station #3 controls the rf systems for DTL tank1 to DTL tank3, while Station #4 controls the final two DTL tanks. The reference signal for the two control stations comes from the RFQ via two RF cables in parallel. The cables are a combination of RF-58 and RG214 cables, which are sensitive to the ambient temperature with respect to phase drift. The parallel signal path also enhanced the differential phase drifts for DTL tanks. The reference signal path has been modified to a single Andrew FSJ1-50A cable, which is phase stable to temperature, from the RFQ to DTL and split at Station #3 to Station #4 as they are located close to each other. In phase measurements, RF noises and side bands were found in the reference signal in the 35 MHz frequency multiplier board. The control board has been replaced and the noise is cleared. The above LLRF modifications have been applied in the 2022 winter shutdown, and the system stability has been improved.

## **ISAC-II CHALLENGES**

ISAC-II is the superconducting (SC) linac downstream of ISAC-I after a S-bend beamline. It accepts RIBs at an energy of 1.5 MeV/u and further accelerates to > 6.5 MeV/u for A/q = 6 isotopes or > 16MeV/u for A/q = 2 ions. The SC linac was built in two stages. Phase-I (SCB) consists of five cryomodules. Each cryomodule has four SC quarter-wave resonators (QWR). SCB cavities operate at 106.08 MHz with two optimized beam velocities ( $\beta$ ) at 5.7% and 7.1% of the speed of light. Phase-II (SCC) consists of three cryomodules. The first two modules have six QWRs, while the last one has eight QWRs. SCC cavities operate at 141.44 MHz with geometry  $\beta$  at 11%. All cryomodules have a 9 T SC solenoid in the centre position. ISAC-II cavities operate at the temperature of 4 K. Cavities are specified to run at the accelerating gradient of 6 MV/m to provide 1 MV effective voltage each. The RF power loss on the cavity wall is less than 7 W in the operating regime, while the RF drive is 200 W in the full reflection regime to broaden the bandwidth for control.

Phase-I was commissioned for operation in 2006 [5], while the Phase-II upgrade was completed in 2010 [6]. Based on the accumulated experience and lessons learned from the over 15 years operation, ISAC-II has developed an on-going refurbishment program to overcome operation challenges, to improve the system availability and reliability, and to pursue the long-term goal of establishing reliable

operation beyond 40 MV. Since 2017, around 37 cavities have been available for beam delivery. The total effective voltage has been improved from 31 MV to 39 MV gradually, and the downtime of the beam delivery caused by the RF system and cryomodule failures has been reduced by a factor of 5 and is now maintained below 10 hours/year.

### *Cavity Ancillaries*

The cavity availability is essential to improve and maintain the linac performance. In case that a failed cavity can not be restored on-line, it will stay 'OFF' at least until the linac warmup in the next winter shutdown, or even wait for a few years depending on the priority. The analysis of the cavity failures in ISAC-II identifies that the most vulnerable parts are on the drive side of the cavity. They include the internal RF transmission line, the RF feedthrough and the RF coupler, plus the cavity frequency tuner plate for various reasons.

The original design selected an Andrew 3/8 inch cable (FSJ2-50) as the internal transmission line in the vacuum tank from the RF feedthrough on the lid of the CM to the RF coupler. The black polyethylene (PE) jacket was removed to avoid the material outgassing and the particulate contamination. After years of operation, seven cables had failures, such as melted insulation material and an RF discharge in the connector. Although FSJ2-50 cable is rated for 2 kW average power in the ISAC-II frequency regime, it cannot promise long-term reliability at 200 W in the full reflection regime in vacuum. One cause is the insulation material is foam PE which outgases when it is warmed up by RF power. The RF glow discharge is not an issue at 200 W under atmosphere pressure. But under vacuum, the RF connector creates a 'closed space' inside. The outgassing from the cable is accumulated in the connector. The local pressure increases to the 'optimized' pressure of the RF glow discharge. Consequently, cable breakdown occurs. The issue has been solved by drilling a venting hole on the connector jacket to prevent trapped gases. The other cause is the RF contact loss at the joint between the cable and the connector. Since the cavity operates in the full reflection regime the peak current of the standing wave is equivalent to 800 W average power in traveling wave. A comparison test of maximizing (80%) and minimizing (10%) the RF current at the connector position demonstrated the contact loss is around 8 W at 200 W forward power, which is equal to the RF loss along the cable due to attenuation. As vacuum does not cool the connector by convections to remove the local heating, it enhances outgassing or even melts the insulation material leading to cable failure. As a mitigation FSJ2-50 cable was replaced by 1/2 inch FSJ4-50B cable with 50% higher rated power to provide more tolerance for the RF contact loss. One failure was observed on the thicker cable after 5 years in operation. It was then decided to upgrade the 'normal' RF cable to the hermetic sealed rigid cable, which is specifically designed for the applications under vacuum, such as satellites. The length of the cable was optimized to minimize the RF current at connector and feedthrough. A loop shape was added to provide reasonable mechanical flexibility to reduce the side loads

to the coupler and to tolerate the thermal shrinkage due to cooldown. The rigid cable was installed in the first CM and is in service of operation in 2022. The mechanical and thermal aspects were verified. It has been working well so far on the RF aspect. The proof of the improvement will be available in the next few years.

Along with the rigid cable upgrade, the RF feedthrough on the lid of the CM was upgraded from MDC N-type to the higher rated Kyocera N-type for the long-term reliability. The rigid cable also brought higher side loads to the variable RF coupler. A redesigned coupling loop with non-magnetic cross-roller bearings and symmetric loading mechanics that was developed for SCC was employed in SCB to improve the mechanical motion.

Frequency adjustment of the ISAC-II cavity is done by adjusting a 1 mm thick niobium plate at the bottom of QWR. The tuner plate is driven by a warm servo motor from the top of the CM via a vertical rod and a horizontal lever connecting to the centre of the plate. The joint between the plate and lever assembly was a short rod welded to the tuner plate for SCB. After over a decade's operation, cracks were found at the weld seam on a few cavities, which increased the risk of losing cavities if the crack developed over time. The welded joint was replaced by bolt and nut connection as the mitigation solution.

The upgrades discussed above cannot be completed at once. They have been implemented to CMs through the ongoing refurbishment program to improve the cavity availability and long-term reliability year by year. It takes about six weeks to remove a cryomodule to the clean room, complete the refurbishment and replace back on-line.

### *Field Emission*

A critical challenge limiting the cavity operating performance in ISAC-II is field emission (FE) caused by the particulates on the RF surface in the high electric field region. It increases RF power loss above the FE onset and reduces cavity gradient at the specified 7 W level. The typical  $Q-E_{acc}$  curve of a FE cavity is shown in Fig. 2 in the red colour, and compared to other normal cavities in the same CM. This cavity could operate at 6 MV/m with < 7 W power loss but with voltage in the strong Q-slope regime. This increases RF instability regarding amplitude and phase errors in LLRF for itself and for the neighbour cavities. As a consequence, the FE increases the chance of cavity trips, which leads to RF downtime. FE can trigger MP, which is typically conditioned after the CM cooldown as per the RF procedure. Reappearance of MP barriers extends the required time to restore the tripped cavity. More severe Q degradations caused by FE were observed and will be discussed in the next sub-section.

The cavity operating gradient is optimized based on the downtime analysis. The mitigation solution to avoid instability and downtime from FE is to run the FE cavities below the FE onset. For example, Cavity #2 in Fig. 2 is set at 5 MV/m in the operation. To compensate the reduced performance from FE cavities, other cavities without FE are pushed to higher gradient as required, even exceeding the 7 W limit for good cavities. Routine Q-curve



measurements track the cavity performance and helps set the cavity operating gradient. The year-to-year statistics also monitors FE enhancements due to particulate migration from the dirty sections through the beamline. The measurements are performed at least once a year in ISAC-II after the winter shutdown. More measurements are conducted if there is an obvious degradation or a significant interruption to the cavity. The Q-curve measurement instead of the gradient measurement at 7 W and the RF set-point optimization have been included in the RF procedure since 2017. With the learning curve from the recent operation, the RF downtime has been greatly reduced, and the total effective voltage has been gradually improved.

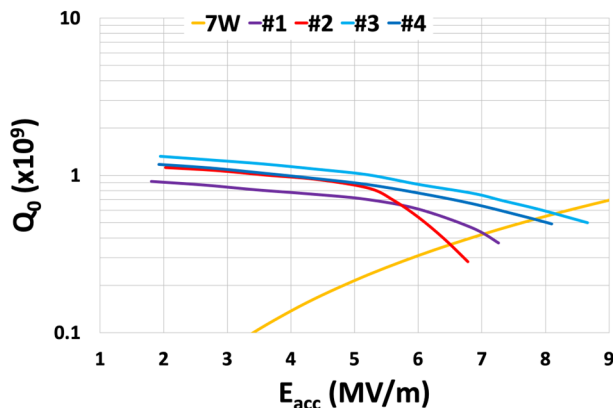


Figure 2: Q- $E_{acc}$  curves of QWRs in a SCB CM.

### Trapped Flux

FE can cause more severe cavity degradation during operation, as shown in Fig. 3. The cavity was set at 6 MV/m in the Q-slope regime on the blue curve. After a cavity trip associated with a significant increase of the helium load, the cavity Q was degraded by one order of magnitude as shown in the red curve. A cavity thermal cycle to the temperature above the SC transition of niobium in the zero magnetic field background restored the cavity performance. It indicated the degradation was caused by a significant amount of trapped flux from the fringe field of the operating solenoid. A recovery procedure (~4 hours) has been developed to restore the linac to operation. The reason of the flux trapping has been mystery for years, as the helium jacket of ISAC-II cavity is made with reactor grade niobium which acts as a Meissner shield for the cavity against the < 1 mT fringe magnetic field in the closet cavity position.

A series of cavity tests were proposed to demonstrate the possibility that the serious degradation is caused by FE and cavity quench. Thermal cycling cavities above the SC transition while maintaining the SC solenoid cold and at 0.5 T field proved that the fringe magnetic field from the solenoid is sufficient to cause a Q degradation by a factor of fifteen. The Q reductions are consistent with the distances from the cavities to the solenoid. A set of intended and aggressive cavity quenches were performed while the solenoid was operating at 4.7 T. In the quench tests, the RF coupler was set in the over coupling regime, but not as strong as that in the operation. The cavity required

20~40 W forward power to quench due to the over coupling. As the amplitude feedback loop in LLRF was closed, after the cavity quenched, the system drove significant higher RF power, controlled by the drive limit in the LLRF, to try to maintain the cavity gradient. The drive limit was adjusted, then an interesting set of data was collected. There was a temperature rising by about 1 K on the cavity bottom before the quench indicated by RF, and it dropped back to the baseline after quench in all quenches. There was no Q degradation after quench when the forward power was limited under 95 W. The first degradation by a factor of ten was obtained at 115 W drive after quench. Additional cavity quench with longer durations in the quench regime further reduced the Q by 50%. An obvious difference was that the cavity top temperature increased by 1~3 K 2 minutes after the cavity quench in the degraded cases, but there were not noticeable changes in the non-degraded cases.

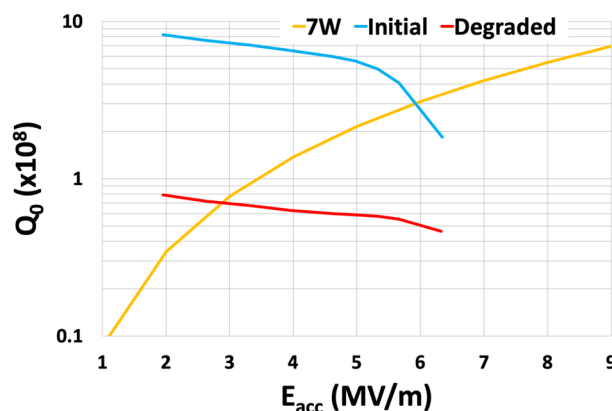


Figure 3: Severe performance degradation of a FE cavity during operation.

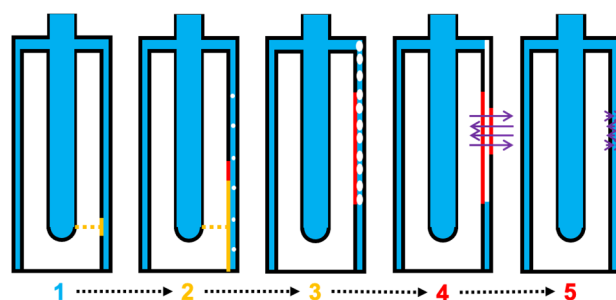


Figure 4: Schematic of the quench development in a FE cavity that finally opens a hole in the Meissner shield and traps flux from the solenoid fringe field.

Based on the above results of the quench tests, a theory of opening a ‘hole’ in the Meissner shield by FE caused cavity quench was developed as shown in Fig. 4. The emitted electrons gain kinetic energy from the RF electric field and impact on the outer conductor. The deposited kinetic energy warms up the cavity bottom. The warm zone grows as FE persists and extends to the higher RF magnetic field zone. The cavity quenches when the local RF magnetic field is sufficient to cause a thermal quench and reduction of RF voltage. As the cavity gradient drops the LLRF increases the drive power to try to maintain the cavity

gradient. At this point, FE disappears, but the thermal quench keeps developing due to  $> 100$  W RF drive. The huge heating power boils liquid helium in the jacket and reduces the cooling efficiency for both the cavity wall and the jacket wall. There are direct thermal paths connecting the cavity wall and the jacket wall through the cavity top plate and the stiffener ring at the middle height of the cavity. The RF heating power at the quench zone is conductively transferred to the jacket, that opens a quench zone on the jacket wall and allows the magnetic flux from the solenoid to enter the Meissner shield. When the RF is off and the cavity cools down, the flux is trapped in both the cavity wall and the jacket wall. The cavity performance does not degrade in the situations #1 – #3 in Fig. 4 but does in #4 and #5. The quench development from #3 to #4 takes about 2 minutes in the quench tests.

More cavity quenches were tested in the zero magnetic field background to restore the Q afterward but did not succeed. The hypothesis is that the significant amount of the trapped flux changes the quench mechanism from FE that caused the initial thermal quench to Ohmic heating. This does not replicate the development process of the previous cavity quench to open a ‘hole’ on the jacket wall. The jacket trapped flux persists in the future quenches. The trapped flux on the cavity wall is re-distributed by quench but cannot be released without a warm-up.

Since the mystery of severe Q degradation was revealed, the avoidance solution has been developed. Operating cavities below the FE onset greatly reduces the opportunity of the FE caused quench. To further protect cavities from unexpected incidences, a quench detection and interlock is required to eliminate this risk. Since the quench takes minutes to open a ‘hole’ on the jacket, an interlock program in EPICS with seconds response time based on the existing cavity diagnostics is sufficient to manage the task.

### Hydrogen in Niobium

ISAC-II QWRs have not been degassed during the cavity manufacture. SCB and SCC cavities were done in different vendors and with different batches of niobium. The high hydrogen content in the niobium of SCC introduces a stronger Q-slope in the medium field regime and limits the cavity performance at 7 W RF loss [7]. The average operating gradient of SCB cavities is 6.3 MV/m, while that of SCC is 5.4 MV/m in 2022. The cause was traced back to the soft vacuum in the electron beam welder in the cavity fabrication. Hydrogen also causes Q-disease when there is a long interruption of the liquid helium supply. Systemic tests show that SCC cavities degrade after 1 hour soaking in the temperature range from 50 K to 200 K, while SCB cavities need 10 hours. Consequently, in the event of a cavity warm-up above 50 K, the CM requires a full room temperature thermal cycle to avoid performance reduction.

To shorten the recovery procedure from days to hours, 600 °C degassing has been proposed in TRIUMF in the next five years plan. A clean ultra-high vacuum furnace will be procured and commissioned to conduct the treatment. As a proof of principle, a SCC cavity was degassed and cold tested. The base Q increased from  $1 \times 10^9$  to  $2 \times$

$10^9$  at 4 K. The medium field Q-slope was also mitigated, and the gradient at 7 W RF loss was improved to 8 MV/m. The SCB cavities will also benefit from the degassing but with less gain expected as compared to SCC. With the hydrogen degassing completion for all ISAC-II cavities, the total effective voltage should gain an estimated 6 MV.

### CM Developments

The SRF team has a CM R&D program for future ISAC upgrades. An ISAC-II style QWR cryomodule with a separated vacuum design has been developed, produced and commissioned at TRIUMF for the energy upgrade of the VECC ISOL-RIB facility [8]. The cavity, RF coupler, frequency tuner and cavity bottom assembly were redesigned to accommodate the hermetic string requirements. The warm-cold transition (WCT), inter-cavity transition (ICT) and multi-layer insulation (MLI) were added to the new design. The successful cryogenic and RF commissioning completed in 2022 verified the functionality of the CM upgrades.

### FUTURE AT ISAC

With the completion of ARIEL, there will be 3 simultaneous RIBs available to ISAC. The current ISAC installations can only provide one accelerated RIB to either the medium or the high energy area. To exploit the full capability of ISAC, a new low energy beamline, a new RFQ and a new low energy CM with 7 QWRs has been proposed to accept RIB from ARIEL, accelerate to ISAC-II and bypass ISAC-I. The parallel accelerator path will allow 2 accelerated RIBs delivered to both the medium and the high energy areas simultaneously. The new accelerator path in ISAC and ARIEL will triple the RIB capability and reach the full power of the RIB programs at ISAC.

The energy upgrade of the ISAC-II linac has also been in the plan. In addition to the cavity performance improvement by hydrogen degassing, a SC booster CM, consisting of 8 QWRs with  $\beta$  at 16%, located at the downstream of SCC3 CM in ISAC-II accelerator vault has been proposed to upgrade the total effective voltage by an additional 16 MV. It will accommodate the higher energy requirement from experimenters and provide flexibility for the RIB operation with a total available voltage of 62MV in total.

As a short conclusion, ISAC linacs have been accelerating RIBs for experiments since 2000. The RF systems have met operation challenges, such as aged critical components and obsolete equipment. On-going refurbishment programs are based on systematic analysis and lessons-learned from two decades of operation. The system’s availability, reliability and capability have been improved by attacking the most vulnerable parts in the RF chain. Development programs and collaborations enhance and augment TRIUMF expertise in Linac technologies for the future.

### REFERENCES

- [1] J. Dilling, *et al.*, “ISAC and ARIEL: the TRIUMF Radioactive Beam Facilities and the Scientific Program”, Berlin, Germany: Springer Dordrecht, 2014.  
doi.org/10.1007/978-94-007-7963-1

- [2] O. Shelbaya, “ISAC-I RF Acceleration”, TRIUMF design note TRI-BN-18-02, 2018.
- [3] R.E. Laxdal, *et al.*, “A Separated Function Drift Tube Linac for the ISAC Project at TRIUMF”, in *Proc. PAC’97*, Vancouver, BC, Canada, May 1997, paper 5W036, pp 1194-1196.
- [4] X. Fu *et al.*, “A Digital Phase-locked Loop Based LLRF System,” in *Nucl. Instrum. Methods Phys. Res., Sect. A* 962 (2020) 163688.  
doi.org/10.1016/j.nima.2020.163688
- [5] R.E. Laxdal *et al.*, “Commissioning and Early Experiments with ISAC-II,” in *Proc. PAC’07*, Albuquerque, New Mexico, USA, Jun. 2007, paper THXAB01, pp. 2593-2597.
- [6] R.E. Laxdal *et al.*, “Operating Experience of the 20MV Upgrade Linac,” in *Proc. LINAC’10*, Tsukuba, Japan, Sep. 2010, paper MO202, pp. 21-25.
- [7] Z. Yao *et al.*, “Operating Experience on Cavity Performance of ISAC-II Superconducting Heavy Ion Linac,” in *Proc. SRF’17*, Lanzhou, China, Jul. 2017, paper TUPB064, pp. 527-530.  
doi.org/10.18429/JACoW-SRF2017-TUPB064
- [8] Z. Yao *et al.*, “Commissioning of the VECC Cryomodule,” presented at LINAC’22, Liverpool, UK, Aug. 2022, paper TUPOGE01, this conference.